Optimum Linear Tapering in the Design of Columns

B. Dinkoff,[1] M. Levine,[1] and R. Luus[2]

Optimum linear tapering of a simply supported solid column enables a saving of 10.4 percent of material, as compared to a nontapered column.

Introduction

We consider the problem of determining the shape of the strongest elastic axially loaded column with simply supported ends. The optimum theoretical shape was obtained by Keller [1] using variational methods and by Taylor [2] using a potential energy approach.

The optimum shape enables a reduction of 13.4 percent in material requirement, but such a column has zero cross-sectional area at the ends. To avoid such a problem, a minimum cross-sectional area constraint was incorporated by Liu [3], Frauenthal [4], and by Foley and Citron [5]. The problem of infinite stress does not arise if the column is clamped as was shown by Tadjbakhsh and Keller [6] and more recently by Olhoff and Rasmussen [7]. Also, if interior supports are used, Olhoff and Taylor [8] showed that the optimal column has finite cross-sectional area throughout.

The aim of this Note is to simplify the formulation and solution of the simply supported column optimization problem by imposing a linear tapering constraint. We shall show that such suboptimal design gives material savings close to the optimum and the problem of infinite stresses does not arise.

Design of Linearly Tapered Columns

Consider a simply supported solid column tapered linearly from the center. Since the weight of the column is neglected, the largest cross-sectional area occurs at the middle of the column to provide the highest moment of inertia for resisting buckling. Given the applied axial load P, the length of the column L, the Young's modulus E, and the shape of the cross section, the problem is to determine the optimum linear tapering of the column so that the total volume of material is minimized and so that the column can withstand the applied load without buckling.

If we let x_0 be the axial distance from an arbitrary reference point to one end of the column, and b be the distance to the middle, the total volume of the column is

$$V = 2\omega \int_{x_0}^{b} [W(x)]^2 dx \tag{1}$$

where ω is the dimensionless area of the cross section chosen. For circular cross section $\omega = \pi/4$, for a square cross section $\omega = 1$, and for an equilaterial triangle, $\omega = \sqrt{3}/4$. $W(x)$ is the cross-sectional dimension, or width, of the column. Since linear tapering constraint is imposed, the width as a function of the axial distance x is

$$W(x) = ax, \quad x_0 \le x \le b \tag{2}$$

Let us denote the dimension of the column at its middle by W_1, so that integration of equation (1) yields

$$V = \omega L \left[W_1{}^2 - \frac{1}{2} L W_1 a + \frac{1}{12} L^2 a^2 \right] \tag{3}$$

The nonbuckling constraint can be formulated by considering the axial deflection y of the slender column on the verge of buckling as given by

$$EI(x) \frac{d^2y}{dx^2} + Py = 0 \tag{4}$$

and the boundary conditions

$$\left.\begin{aligned} y &= 0 \quad \text{at} \quad x = x_0 \\ \frac{dy}{dx} &= 0 \quad \text{at} \quad x = b \end{aligned}\right\} \tag{5}$$

where the moment of inertia is given by

$$I(x) = \xi [W(x)]^4 \tag{6}$$

The dimensionless moment of inertia ξ is introduced to enable different cross-sectional shapes to be used, once the results are obtained for the general case. For circular cross section $\xi = \pi/64$, for square cross section $\xi = 1/12$, and for an equilateral triangle, $\xi = \sqrt{3}/96$.

Substitution of equations (2) and (6) into equation (4) yields

$$x^4 \frac{d^2y}{dx^2} + \alpha^2 y = 0 \tag{7}$$

where

$$\alpha^2 = \frac{P}{E\xi a^4} \tag{8}$$

If we let

$$x = 1/\theta \tag{9}$$

equation (9) can be converted into the Bessel equation

$$\frac{d^2y}{d\theta^2} + \frac{2}{\theta}\frac{dy}{d\theta} + \alpha^2 y = 0 \tag{10}$$

With the further substitution

$$z = y\theta \tag{11}$$

equation (10) becomes a linear differential equation with constant coefficients

$$\frac{d^2z}{d\theta^2} + \alpha^2 z = 0 \tag{12}$$

which is readily solved with the boundary conditions of equation (5) to give

$$\tan \left[\frac{\alpha}{b} - \frac{\alpha}{x_0} \right] - \frac{\alpha}{b} = 0 \tag{13}$$

or

$$\tan \left[\frac{k}{W_1 a} - \frac{k}{a\left(W_1 - \frac{L}{2}a\right)} \right] - \frac{k}{aW_1} = 0 \tag{14}$$

where

$$k = \sqrt{\frac{1}{\xi}\frac{P}{E}} \tag{15}$$

This is equivalent to

$$\phi(a, W_1) = \frac{k}{W_1 a} - \frac{k}{a\left(W_1 - \frac{L}{2}a\right)} + \pi - \tan^{-1}\left(\frac{k}{aW_1}\right) = 0 \tag{16}$$

which is more convenient than equation (14) since $\tan^{-1}$ function is bounded. The term is included to insure the correct region for the periodic $\tan^{-1}$ function in the range of realistic values for a and W_1. Equation (16) provides the necessary constraint for a and W_1 at the verge of buckling of the column.

[1] Students, Division of Engineering Science, University of Toronto, Toronto, Ontario M5S 1A4, Canada.

[2] Presently (from September 1, 1979 to June 15, 1980), Department of Chemical Engineering, California Institute of Technology, Pasadena, Calif. 91125.

Manuscript received by ASME Applied Mechanics Division, March, 1979; final revision, July, 1979.

Table 1 The optimal dimensions of a linearly tapered column for a variety of given parameters

GIVEN PARAMETERS					OPTIMAL DIMENSIONS					
P, kN	L, m	E, GPa	ω	ξ	a	W_o, m	W_1, m	V, m^3	$\frac{aL}{W_1}$	$\frac{V}{V_n}$
10	2.5	10	1.0	$\frac{1}{12}$ *	0.02092	0.03606	0.06221	0.006178	0.8408	0.8965
35	3	25	1.0	$\frac{1}{12}$	0.02078	0.04297	0.07413	0.01053	0.8408	0.8965
50	4	30	$\sqrt{3}/4$	$\frac{\sqrt{3}}{96}$ **	0.02755	0.07598	0.1311	0.01900	0.8408	0.8965
75	5	120	$\sqrt{3}/4$	$\frac{\sqrt{3}}{96}$	0.01928	0.06647	0.1147	0.01818	0.8408	0.8965
90	5	70	$\pi/4$	$\frac{\pi}{64}$ ***	0.01798	0.06198	0.1069	0.02868	0.8408	0.8965
120	7	40	$\pi/4$	$\frac{\pi}{64}$	0.01878	0.09064	0.1564	0.08585	0.8408	0.8965

* corresponds to square cross-section

** corresponds to equilateral triangular cross-section

*** corresponds to circular cross-section

Minimization of Volume Subject to Buckling Constraint

Minimization of the volume, V, given by equation (3) subject to the buckling constraint specified by (16) is equivalent to the minimization of the augmented performance index

$$J = V + \lambda\phi(a, W_1) \tag{17}$$

where the buckling constraint in equation (16) is appended by the Lagrange multiplier λ. The necessary conditions for minimum of J are the stationary conditions

$$\left.\begin{aligned} \frac{\partial J}{\partial a} &= 0 \\ \frac{\partial J}{\partial W_1} &= 0 \end{aligned}\right\} \tag{18}$$

We are thus led to find the variables a, W_1, and λ such that equations (16) and (18) are satisfied. This set of nonlinear equations can be solved numerically in a straightforward manner by Newton's method where the initial values are chosen at random as suggested by Luus and Jaakola [9]. The minimization was performed for various different values of P, L, E, and shape of cross section. In each case convergence was very rapid, yielding 0.001 percent accuracy within 10 iterations.

For the various combinations of P, L. E, and cross section used, two relationships were established from the optimization runs, some of which are reported in Table 1, namely,

$$\frac{aL}{W_1} = 0.8408 \tag{19}$$

and

$$\frac{V}{V_n} = 0.8965 \tag{20}$$

where V_n is the minimum volume of material required in the equivalent nontapered solid column to withstand the load without buckling,

$$V_n = \omega L^2 \sqrt{\frac{1}{\xi}\frac{P}{\pi^2 E}} \tag{21}$$

From equation (20) it is seen that the percent saving of material through optimum linear tapering is 10.4 percent as compared to the corresponding nontapered column. It is interesting to note that the material saving for an optimally tapered column is independent of P, L, E, and cross-section shape.

Since

$$\frac{aL}{2} = W_1 - W_0 \tag{22}$$

it follows from equation (19) that with optimum linear tapering

$$\frac{W_0}{W_1} = 0.5796 \tag{23}$$

Thus the cross-sectional dimension at the ends of the column is about one-half the corresponding distance in the middle of the column, and infinite stress concentrations do not occur. The optimum distance at the center is

$$W_1 = 1.1849 \sqrt[4]{\frac{1}{\xi}\frac{PL^2}{\pi^2 E}} \tag{24}$$

so the shape of the optimal linearly tapered column is immediately obtained. The column is easy to construct and a 10.4 percent material saving can be realized. This saving is reasonably close to the 13.4 percent saving determined for the optimum theoretical column shape.

Discussion and Conclusions

The optimal linearly tapered column is compared to the theoretical optimum column shape and other suboptimal designs in Fig. 1. The design based on Frauenthal's formulation leads to a material saving of 11.8 percent. For direct comparison, the maximum stress was specified to be the same as that encountered at the ends of the optimally linearly tapered column and the method of Luus and Jaakola [10] was used for optimization. It is noted that at 0.0675 L from either end a pronounced change in the shape of the column occurs.

It is interesting to note that with optimal linear tapering the ratio W_0/W_1 is constant for all P, L, E, and cross-section type.

Acknowledgment

This investigation was supported in part by the National Research Council of Canada under Research Grant A-3515. The computational facilities of the University of Toronto were used for the numerical results.

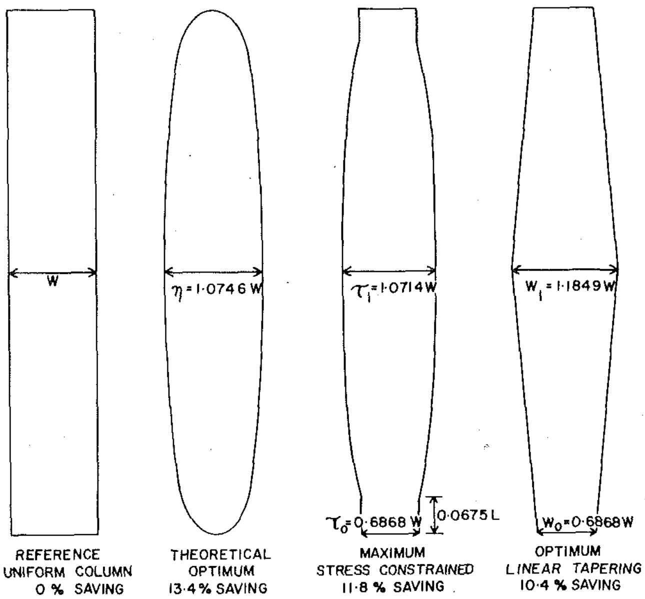

Fig. 1 Comparison of theoretical optimum column shape to various suboptimal designs.

References

1 Keller, J. B., "The Shape of the Strongest Column," *Arch. Rational Mech. Anal.*, Vol. 5, 1960, pp. 275–285.

2 Taylor, J. E., "The Strongest Column: An Energy Approach," ASME JOURNAL OF APPLIED MECHANICS, Vol. 34, No. 2, 1967, pp. 486–487.

3 Taylor, J. E., and Liu, C. Y., "Optimal Design of Columns," *Journal of the American Institute of Aeronautics and Astronautics*, Vol. 6, No. 8, 1968, pp. 1497–1502.

4 Frauenthal, J. C., "Constrained Optimal Design of Columns Against Buckling," *Journal of Structural Mechanics*, Vol. 1, No. 1, 1972, pp. 79–89.

5 Foley, M., and Citron, S. J., "A Simple Technique for the Minimum Mass Design of Continuous Structural Members," ASME JOURNAL OF APPLIED MECHANICS, Vol. 44, 1977, pp. 285–290.

6 Tadjbakhsh, I., and Keller, J. B., "Strongest Columns and Isoperimetric Inequalities for Eigenvalues," ASME JOURNAL OF APPLIED MECHANICS, Vol. 29, 1962, pp. 159–164.

7 Olhoff, N., and Rasmussen, S. H., "On Single and Bimodal Optimum Buckling Loads of Clamped Columns," *International Journal of Solids and Structures*, Vol. 13, 1977, pp. 605–614.

8 Olhoff, N., and Taylor, J. E., "Designing Continuous Columns for Minimum Total Cost of Material and Interior Supports," *Journal of Structural Mechanics*, Vol. 6, 1978, pp. 367–382.

9 Luus, R., and Jaakola, T. H. I., "Optimization of Nonlinear Functions Subject to Equality Constraints. Judicious Use of Elementary Calculus and Random Numbers," *I & EC Process Design and Development*, Vol. 12, 1973, pp. 380–383.

10 Luus, R., and Jaakola, T.H.I., "Optimization by Direct Search and Systematic Reduction of the Size of Search Region," *AIChE Journal*, Vol. 19, No. 4, 1973, pp. 760–766.

Resonance Method for Identifying Fluids Filling Cavities in Elastic Solids

G. Gaunaurd[1] and H. Überall[1,2]

Introduction

When compressional waves traveling through elastic (possibly sound-absorbing) solids are incident on a fluid-filled spherical cavity in the medium, a compressional *and* a shear wave are scattered from it. We have studied [1] the backscattering amplitudes of the returned waves in the light of a new theory of viscoelastic wave-scattering. The initial success of this theory rests on the fact that the partial-wave contributions making up the obstacle's cross section can be split into two interfering parts. This decomposition already provides much physical insight into the scattering mechanism taking place around the cavity. These contributions are the smooth ("potential") backgrounds associated with echoes from an evacuated cavity, and the interacting discrete resonances of the filler. The scattering amplitudes of the returned compressional and shear waves were shown, respectively, to have the same resonances. This observation simply means *that since the resonances are a (characterizing) property of the filler,* they are equally communicated by the obstacle to both types of scattered waves, but with different strengths. Further success of this theory is based on the frequency and mode-order interpretation of the isolated resonances in terms of creeping waves circumnavigating the cavity [2]. This provides additional physical interpretation of the scattering process in terms of related observable surface-wave phenomena, as well as insight into properties of the S-matrix and its associated ("Regge") poles. In the foregoing, the modal resonances (i.e., fundamental $l = 1$, and overtones $l = 2, 3, \ldots$, for each mode n) are found by subtracting suitable background from the composite modal contributions, and then displaying the so modified respective scattering amplitudes versus either wavesize ka, or mode order n. The resulting resonance "lines" have widths and the concept of line width is as useful here as its analogue was originally in optical spectroscopy. Once the modal resonances have been (computationally) isolated we will show how one can quickly find from their location, widths, and spacings, the complete material characterization of the filler as if we were looking at its signature. This is the central idea of the present paper. We will specifically show that the locations and spacings of all the resonances of any given mode determines the filler/matrix wavespeed ratio, while the widths Γ_{nl} of any of the l resonances of any mode and their spacing, will furnish the filler/matrix density ratio. If the matrix properties are known, the aforementioned ratio determination fixes the filler properties and vice versa. The filler is assumed fluid for simplicity and in order for our earlier work [1, 2] to apply directly without modifications. The fluid-filler is completely identified once its density and sound speed are determined by our simple asymptotic process.

Theory

(*a*) Determination of the Filler/Matrix Sound Speed Ratio. We found [1, equation 16] that the complex eigenfrequencies of the filler-fluid were given by the zeros of a 3×3 determinant denoted D_n and whose complex elements d_{ij} were all given before [1]. The real resonance frequencies are the real parts of these eigenfrequencies. The physical situation of a fluid-filled cavity in a metal, allows us to reduce the eigenfrequency condition $D_n = 0$ to the simpler form $d_{13} = 0$. The McMahon [3] expansion for the roots of this equation is

$$(k_f a)_{n,l} = \left(l + \frac{n}{2} - \frac{1}{2}\right)\pi - \frac{(2n+1)^2 + 7}{8\pi\left(l + \frac{n}{2} - \frac{1}{2}\right)} \cdots \left(\begin{matrix} l \gg 1 \\ n, \text{fixed} \end{matrix}\right) \qquad (1)$$

where $k_f = \omega/c_f$, c_f = sound speed in the filler-fluid and ω = circular frequency of the incident compressional wave. In terms of $k_d a \equiv x$ ($k_d = \omega/c_d$), c_d = dilatational speed in the elastic matrix, and a = cavity

[1] Research Physicists, Code R-31, Naval Surface Weapons Center, White Oak, Silver Spring, Md. 20910.

[2] Also at the Physics Department, The Catholic University, Washington, D. C. 20064.

Manuscript received by ASME Applied Mechanics Division, December, 1978; *final revision, July, 1979.*